



Regular Article

Identifying urban prone areas to flash floods: The case of Santa Cruz de Tenerife

Nerea Martín-Raya^{*}, Jaime Díaz-Pacheco, Pedro Dorta Antequera, Abel López-Díez

Land planning and Risks Research Group (GEORIESGOS), Chair on Disaster Risk Reduction and Resilient Cities, University of La Laguna (ULL), San Cristóbal de La Laguna, Tenerife, Spain

ARTICLE INFO

Keywords:

Urban sprawl
Flood susceptibility
Original drainage basin
Hydrologic modeling

ABSTRACT

Floods are the natural hazard that causes the largest annual losses in the world. Urban expansion and population growth have made cities the most hazardous areas, mainly due to poor planning, occupation of the drainage network and soil sealing. Santa Cruz de Tenerife is one of the many cities worldwide threatened by this phenomenon. Its typically Mediterranean rainfall pattern, characterized by extreme precipitation events in short periods of time, together with its orography of steep ravines, short length and width, as well as its disorderly growth, make it a space prone to the occurrence of flash floods. In addition, the increase in torrential rainfall as a consequence of climate change and the tendency towards greater irregularity in precipitation is considerably intensifying the problem. This paper studies the characteristics of these episodes and the black spots inventoried in its General Management Plan (PGO for its initials in Spanish). On the other hand, flood modeling is carried out based on the rainfall characterization, whose maximum flows, in total, range between 500 and 1600 m³/s. Finally, a methodology that allows integrating both analyses to obtain a detailed hazard map is proposed as an alternative to the more traditional flood hazard analyses. A design storm of 288 mm is applied and the data is validated against the largest rainfall event on record, March 31, 2002. It has been shown that in an urban drainage network, the main watercourses and those that have disappeared due to urbanization represent areas susceptible to flooding and are the sectors that should be emphasized during the implementation of risk reduction measures. Finally, emphasis is placed on the need to integrate future climate projections of precipitation to better define the maximum flood flows.

1. Introduction

Floods, on a global scale, are considered the most common and devastating natural hazards [1]. These cause around 5000 fatalities and significant material and economic damage each year [2]. In many mountainous volcanic islands, the most frequent are flash floods, which, due to the small capacity of the basins and the slope of the terrain, occur suddenly, linked to runoff processes and in a short period of time. Therefore, they are difficult to predict [3,4]. Furthermore, this type of flooding is also typical of arid or semi-arid environments in coastal areas, with nearby mountain systems, where small basins flow and the riverbeds are dry most of the year, as is the case of the Mediterranean coast, the southeastern USA or southern Brazil [5–8].

The linkage of floods with hydrometeorological phenomena, which with a high level of confidence will continue to increase in intensity and

magnitude in the current context of climate change [9], coupled with increased exposure in areas of high susceptibility and hazard has greatly aroused interest in analyzing the causes that may be raising the risk against this type of hazard [10–15]. Indeed, the increase in heavy rainfall may be one of the drivers. In fact, it is estimated that, over the last decade, one in four precipitation records can be attributed to climate change [16]. As with other hazards, there has been a considerable increase in losses and damages caused by floods [17]. However, beyond climate change, the most important factor in this trend is the increase in exposure and vulnerability, even more so than the change in rainfall patterns. The increase in population and urban growth in many sectors of the planet have made thousands of people more vulnerable to this hazard on a daily basis. In fact, there is a strong correlation between urban sprawl and increased flood risk [18] mainly because increased soil impermeability and decreased infiltration lead to more frequent and

^{*} Corresponding author.

E-mail addresses: nmartir@ull.edu.es, nmartinr@ull.edu.es (N. Martín-Raya), jdiazpac@ull.edu.es (J. Díaz-Pacheco), pdorta@ull.edu.es (P. Dorta Antequera), alopezd@ull.edu.es (A. López-Díez).

<https://doi.org/10.1016/j.pdisas.2024.100372>

Received 28 April 2024; Received in revised form 11 September 2024; Accepted 16 September 2024

Available online 18 September 2024

2590-0617/© 2024 Published by Elsevier Ltd. This is an open access article under the CC BY-NC-ND license (<http://creativecommons.org/licenses/by-nc-nd/4.0/>).

severe flooding [19]. Thus, the effects of drainage density and soil sealing on localized runoff in urbanized areas have been extensively studied [20–24]. Nonetheless, most of the studies that have undertaken the characterization of flooding have focused on the parameterization and modeling of the rainfall regime and its territorial specialization, sometimes omitting aspects more closely related to other factors such as exposure and vulnerability derived, for example, from urbanization processes [25].

Urbanization exacerbates the territorial impacts caused by floods, however, the specific causes that generate them still need to be investigated in depth [26,27]. Especially because, although there are parallels between the places where they occur, there are always local factors, such as slope, topography, types of settlements or hydraulic infrastructure capacity, that need to be analyzed to improve risk management at these scales.

In this sense, although in the analysis of flood hazard the estimation in terms of intensity and spatial-temporal magnitude of the drivers are key (intense rainfall, stream flooding, tropical storms, storms, melted snow, etc.), the identification of prone areas play a huge role for risk management. Therefore, informal urbanization processes or inadequate planning are a clear example of factors involved in the dynamics of flood hazard through the alteration of natural watercourses through which water was previously evacuated with a lower probability of flooding exposed elements.

In this context, this paper analyzes the causes involved in the flood hazard in the city of Santa Cruz de Tenerife in the Canary Islands. A large urban area in the context of the island region where it is located (205,000 inhabitants), which suffered a flood disaster at the beginning of the century (2002) that caused great economic losses and even the loss of human lives, and where this type of phenomena shows a significant degree of recurrence [28]. The study analyzes flood susceptibility for the entire urban area. Empirical-statistical models currently exist that focus on considering and identifying black spots for susceptibility analysis [29,30]. However, these do not go so far as to combine with the widely developed physico-numerical models [31–33] as both methodologies are always developed separately [34]. For this purpose, this study combines the use of a traditional model of hydraulic analysis of flow behavior in the basins with an empirical model based on the history of local impacts in order to detail and improve the identification of areas prone to flash floods. This allows to identify the causes, which are not always linked to the overflowing of watercourses, but are directly related to processes of runoff and deficiencies on the urban drainage. In total, more than 1000 damage points recorded during historical flood events are analyzed and the causes that may be generating the high susceptibility of these areas to flood hazards are established. The results show that, in more than half of the cases, the impacts are related to watercourse and stream overflows. It also points out that a significant percentage of these impacts are related to urban drainage problems and runoff processes. It should be noted that this work does not describe other common and important factors in disaster risk reduction, such as socioeconomic factors, because the objective is focused on analyzing and developing a hazard map to identify areas susceptible to flooding and not on conducting a complete risk analysis.

2. Study area

The selected study area has been defined according to the administrative limits of the municipality of Santa Cruz de Tenerife, since the natural boundaries of the basins include other municipalities in which there are no damage point records. The zone with the highest urban density has been selected, excluding a large part of the municipal surface that corresponds to an extensive protected natural area, which includes small rural settlements that do not form part of the urban continuum of the central city. To the southwest, the study area is circumscribed by the administrative limits of the municipality and to the northeast the limitation follows the border of the hydrographic basins that affect the urban

continuum (Fig. 1).

This main urban area is located mostly to the SW on a moderately slope formed by the accumulation of volcanic materials from the Pedro Gil Rift through which the municipality's large ravines run. To the NE, the expansion of the city is limited by the Anaga Massif, a very abrupt relief of greater geological antiquity. This area is home to small basins with well embedded watercourses, whose lower sections contain urban settlements that, together with the hillside neighborhoods, often suffer damage during the flash flood events.

Santa Cruz de Tenerife is the municipality of the island most affected by flooding episodes and, due to its high population and geographical location, the most exposed to flooding. The Spanish Ministry of Ecological Transition and Demographic Challenge [35] has centralized the information prepared by the Spanish hydrographic basins related to floods, according to the European Commission's Flood Directive 2007/60, delimiting flood zones. These are the areas with significant potential risk of flooding (ARPSIs). In the case of the island of Tenerife, eight have been detected. Of these, 3 are located in Santa Cruz de Tenerife, which gives an idea of its high risk of flooding, which is also confirmed by the fact that it concentrates the highest number of recorded events of this type [36]. In recent decades, it has suffered several particularly serious flooding episodes and has been directly affected by three of the most important precipitation events of the 21st century: March 2002 and February 2010 and October 2014. The rains of March 31, 2002 were the episode with the highest hourly intensity (160 mm/h) and volume of precipitation (232.6 mm) of the series. During the event there were significant damages, 8 victims and the losses compensated by the Insurance Compensation Consortium (*Consortio de Compensación de Seguros*) amounted to 43 M€ [37].

2.1. Rainfall patterns and precipitation extremes

The rainfall patterns of the Canary Islands are similar to those of the Mediterranean world. As such, it has a series of characteristics, the most notable of which are, firstly, a marked seasonality, with maximum rainfall concentrated in the cold months (from November to March) and with a marked summer drought. Secondly, in general, precipitation is scarce, but with large geographical differences, so that rainfall varies, approximately, between 1500 mm per year in the rainiest sectors versus 100 in the driest ones [38]. Thirdly, one of the most defining features of rainfall in this southeastern region of the North Atlantic is its great rainfall irregularity, with coefficients of variation ranging between 30 % and 70 %, the highest in Spain and probably among the highest in Europe (Fig. 2). Finally, fourthly, as in all regions with Mediterranean precipitation regimes, there is a high hourly intensity with a high temporal and spatial concentration of rainfall. Therefore, the data for the Canary Islands exceed 0.63 in the daily precipitation index (CI) designed by Martín Vide in 2004 [39,40].

In the case of Santa Cruz de Tenerife, the average annual rainfall in the city barely reaches 230 mm. The coefficient of variation is around 40 %, so that very dry years alternate with very rainy years, with occasional episodes of torrential rainfall being common. The latter are the ones that trigger flooding events that have caused significant human and material damage. The estimated economic losses caused by floods in the last 20 years amount to 122.3 million euros, and conform, throughout the Canary Islands archipelago, as the second phenomenon of climatic origin in damages, only surpassed by marine storms [37]. Since 1950, the year in which data began to be collected quantitatively, more than 20 episodes of flooding have been recorded in Tenerife [41].

The rainfall pattern is not the only condition that favors the occurrence of floods. The municipality's orographic conditions are key and determining factors. In Santa Cruz de Tenerife there are three sectors with distinct topographic, geological and morphohydrological characteristics (Fig. 1). The northern sector of the old Anaga Massif, with small basins (most of them smaller than 3 km²), and where runoff, if it occurs at all, suffers a certain delay with respect to precipitation due to the high

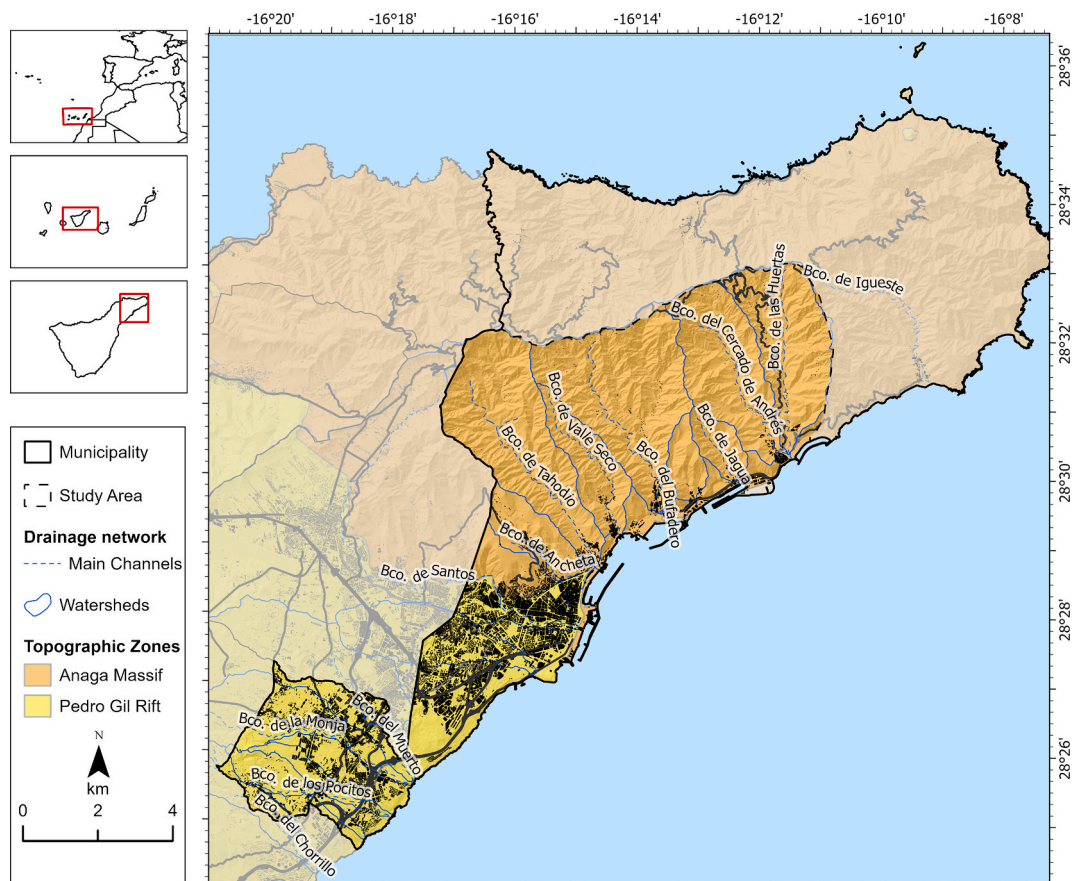


Fig. 1. Location of the study area.

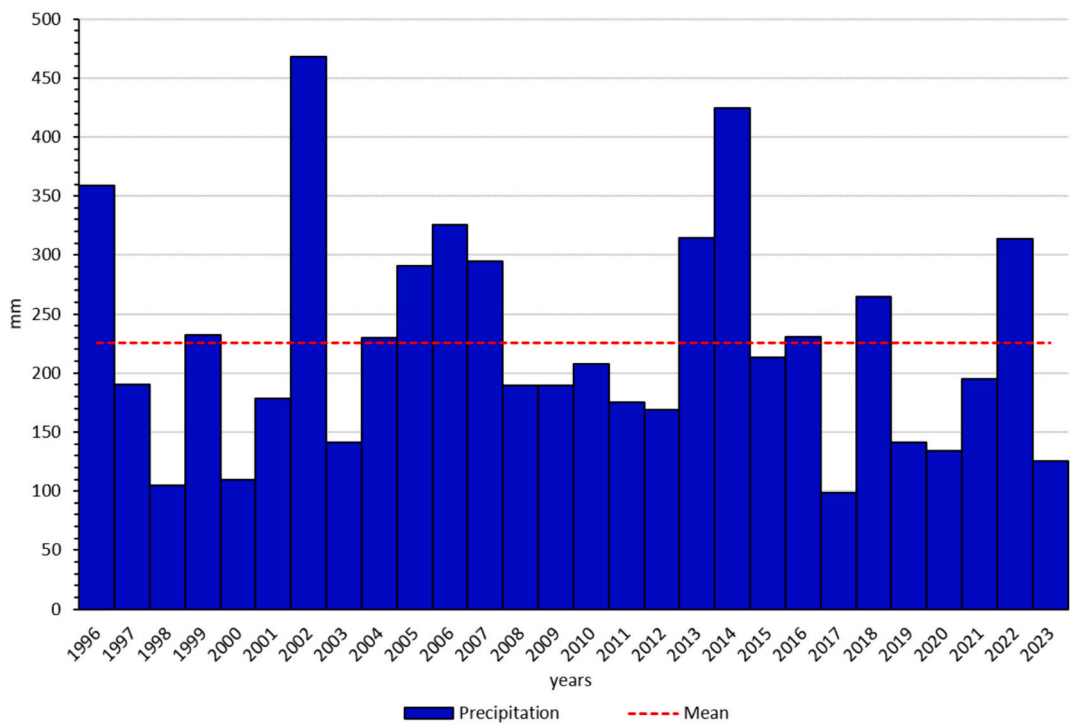


Fig. 2. Annual precipitation in Santa Cruz de Tenerife (1933–2023).

drainage capacity and the absence of important population settlements. On the other hand, in the southern sector of the same massif, the ravines are characterized for being deep, short and with steep slopes. This sector contains the largest and most developed basins (10–15 km²). Finally, the south-western sector of the municipality comprises a much gentler relief composed, for the most part, of a lava ramp, with ravines and incisions of scarce entity arranged in parallel and with underdeveloped headwaters due to its geological youth associated with the formation of the Pedro Gil volcanic ridge.

3. Methodology and sources

This research develops a deductive quantitative methodology that aims to delimit the areas of greatest susceptibility to flooding in the city of Santa Cruz de Tenerife. Traditionally, flooding analysis of cities is performed from hydraulic and hydrological modeling of the study area [42] where, from the use of programs such as HEC-RAS or IBER, simulations are performed showing floodable areas and water draughts [43–45]. However, the level of urbanization and consequent imperviousness of the soil in today's cities leads to a limitation in the susceptibility analysis when relying solely on the modeling of existing watercourses. This is because these do not take into account the direct runoff that occurs outside the channels themselves, as a consequence of the lack of drainage, poor sewerage management, the occupation of old channels, or even hillside runoff [46]. Therefore, to delimit the most susceptible sectors in the city it is not only necessary to pay attention to what happens in the watercourses themselves, but also in other locations where, when high intensity hourly rainfall occurs, it is common to record incidences or problems [47–49].

This paper applies a methodology that integrates all these issues to obtain a susceptibility model more appropriate to the geographic and urban reality of this type of urban areas. For this purpose, a systematic process that sequentially analyzes the causes that increase the susceptibility to flooding has been carried out. This process is organized in five stages.

3.1. Stage 1. Identification of historical modifications to the natural drainage network

During urban expansion processes, the natural drainage network is modified; watercourses are occupied with infrastructure and buildings, streams are canceled and flow transfers are made from some watercourses with no provision for extreme situations. This is especially the case in frameworks where land-use planning policies only superficially consider flood risk management, at least for implementation purposes. This is the case of the urban expansion of Santa Cruz de Tenerife, especially that which took place during the last century, as occurred in many Spanish cities. The municipality suffered from a rather lax planning regarding flood risk management policies through land use planning. In fact, despite the succession of different land laws and instruments that could exert control to curb the occupation of flood-prone areas, it was necessary to wait until 2008. A true territorial perspective is then applied to flood risk management policies throughout the State. It was from the legislative transposition of the European Directive 60/2007, when a binding flood risk mapping on land use planning began to be developed [50]. Hence, the identification of the original drainage network, prior to periods of major development of the urban fabric in cities, is essential for a detailed and complete susceptibility analysis [51]. In fact, spaces where watercourses were occupied or disappeared under the growth of cities continue to function as watercourses and drainage lines during extreme episodes of precipitation [52].

The identification of watercourses that have been buried or modified by the urban fabric is an investigation that combines the analysis techniques of Geography and History, especially when it is carried out on past periods where the lack of accurate sources is a recurrent issue. Older

cartography, aerial photographs and, in more recent times, satellite remote sensing images can help to construct the original drainage network of the space now occupied by a city [53]. In the case of this paper, it was possible to obtain the hydrographic network that the city had around the first half of the twentieth century. By then, the urban fabric occupied 1/3 of the current space. The cartographic source that has been used are the Minutes of the National Topographic Map of Spain [54], which began to be made by photomechanical reproduction techniques, from 1915 to 1960. This technical cartography was prepared at a scale of 1:25,000 and is kept in the IGN Map Library [55].

Using the WMS 1.3.0 Service according to ISO 19128:2005, the natural hydrographic network that functioned before the expansion of the city after 1950 was digitalized.

3.2. Stage 2. Identification of damage incidents recorded in historical flood episodes in the city

Inductive methods to analyze flood hazard in urban environments include the identification of hot spots and areas of verified impact [56]. To meet this objective, an inventory of damage incident points produced by historical flood event impacts was used in the risk study of the General Management Plan of the city of Santa Cruz de Tenerife [57]. This study, among other events prior to the year of the drafting of the plan, mainly included the impacts of the 2002 Santa Cruz de Tenerife flood. In this risk study linked to the municipality's management plan, an exhaustive study was carried out to identify the hot spots by means of a thorough territorial analysis of past events, drainage works and previous research, as well as surveys of the public administrations involved.

For this research, a process of digitalization of the points to a geographic information system was carried out, transferring the classification of the impacts according to the PGO: (1) lack of or insufficient drainage capacity, (2) incorporation of sediment, (3) obstruction of the drainage network and (4) danger of overflowing. A basic statistical-descriptive analysis was performed with these categories.

3.3. Stage 3. Relationship between recorded damage incidents and historical modifications of the natural drainage network

In order to find relationships between recorded damage incidents and historical modifications of the natural drainage network, a 100 m buffer is generated from the watercourse bed to locate impacts that may have some kind of link with the modification of the drainage network. Next, a comparative analysis is carried out between the type of incident located in the area of influence of the missing streams versus those located near the current drainage network.

3.4. Stage 4. Hydraulic modeling based on precipitation and flow extremes

Hydraulic modeling, as a method for flood risk analysis, is widely used at a global scale [58]. It is usually presented as a sequential methodology where it is necessary to identify precipitation extremes and their respective return periods in order to subsequently calculate design flows and model flood zones. The complexity of this phase of the research is such that it is subdivided into 3 distinct and sequential sections: (1) calculation of return periods and estimation of IDF curves; (2) estimation of flows for an extreme precipitation event; and (3) modeling of the behavior of the basins for the estimated extreme precipitation scenario.

3.4.1. Calculation of return periods and intensity-duration-frequency curves (IDF)

The first step to perform a rainfall analysis of the city of Santa Cruz de Tenerife entails obtaining the return periods and their respective IDF curves [59]. In this case, the initial information used corresponds to the ten-minute data recorded between 1996 and 2022 at the Santa Cruz de

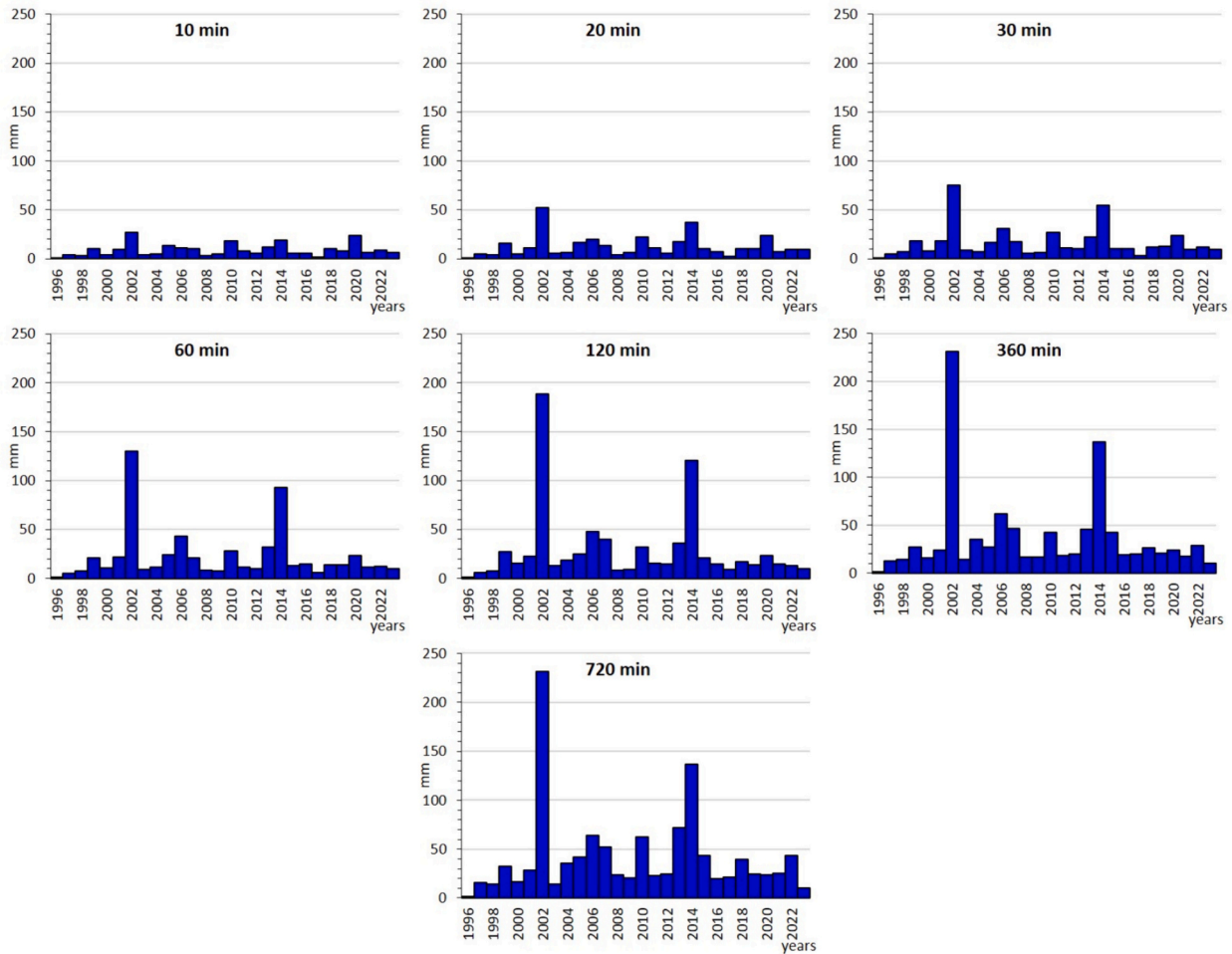


Fig. 3. Maximum annual precipitation in each time interval.

Tenerife station (C449C), belonging to the Spanish State Meteorological Agency (AEMET for its initials in Spanish). From them, the maximum annual precipitation is obtained for the following time intervals: 10, 20, 30, 60, 60, 120, 360 and 720 min (Fig. 3) and then, through Gumbel III, the return periods (2, 5, 10, 25, 50, 50, 100, 250, 500 and 1000 years) are calculated for each time window. Finally, the precipitation obtained is converted to mm/h units to make the IDF curves.

3.4.2. Flow estimation

The unit hydrograph method proposed by the Soil Conservation System (SCS) [60] is used for flow calculation. In this case, as a design storm, an event of 2 h duration in a return period of 500 years (T500) has been considered and the total precipitation for this duration in 20-min intervals has been obtained from the IDF curves. In this sense, the accumulated and produced precipitation in each interval (Fig. 4) is obtained and subsequently, the latter is reorganized through the methodology of alternating blocks [61] to obtain the hietogram.

The calculation of peak discharges (Q_{500}) is performed by using HEC-HMS (Hydrologic Modeling System), a software designed to simulate the complete hydrological process of a basin. In order to obtain the flow rates by the method used, it is necessary to know, in addition to the precipitation hietogram, the Manning coefficient, the curve number and the lag time of each of the basins to be analyzed. The first two variables were obtained from the methodological guide for the development of the National Flood Zone Mapping System (SNCZI for its initials in Spanish) [62]. Here, Manning’s values are pre-established according to the land uses recorded by the Corine Land Cover (Table 1). On the other hand, the curve number is calculated as follows:

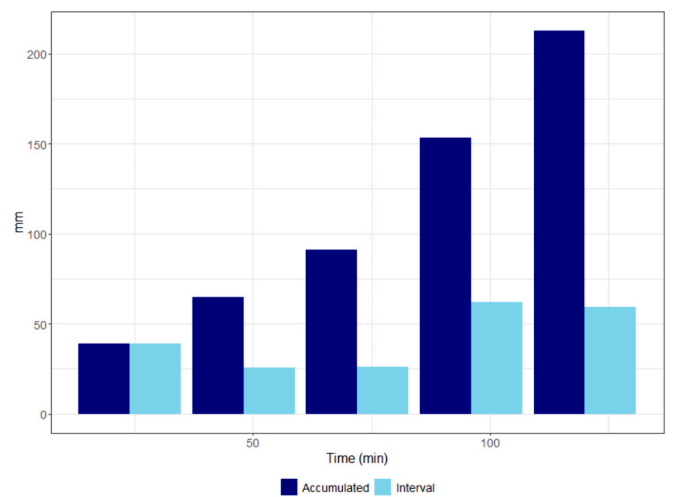


Fig. 4. Interval and accumulated precipitation for T500 in Santa Cruz de Tenerife.

Table 1
Initial parameters of the study basins.

| Basin | L (km) | Sw (%) | Tlag (min) | CN | Manning |
|----------------|--------|--------|------------|-------|---------|
| Cueva Bermeja | 3.20 | 29.38 | 23.07 | 80.00 | 0.03 |
| Jagua | 2.08 | 33.21 | 13.95 | 83.00 | 0.03 |
| Las Huertas | 5.78 | 15.03 | 61.85 | 74.00 | 0.04 |
| Los Pocitos | 4.50 | 37.05 | 23.68 | 84.00 | 0.07 |
| Ofra | 7.40 | 6.89 | 65.40 | 90.00 | 0.09 |
| Santos | 14.10 | 6.97 | 150.10 | 81.00 | 0.06 |
| Tahodio | 8.10 | 13.71 | 89.72 | 72.00 | 0.04 |
| Valleseco | 5.23 | 16.07 | 52.14 | 76.00 | 0.04 |
| Bufadero | 6.67 | 14.29 | 71.14 | 74.00 | 0.04 |
| Cercado Andrés | 4.91 | 19.04 | 46.80 | 75.00 | 0.04 |
| Chorrillo | 10.57 | 12.30 | 120.47 | 71.00 | 0.05 |
| Muerto | 11.80 | 17.23 | 82.92 | 81.00 | 0.06 |
| Pilar | 5.50 | 28.54 | 27.43 | 88.00 | 0.05 |
| Grande | 8.60 | 11.92 | 72.52 | 83.00 | 0.06 |
| Barrio Nuevo | 2.23 | 39.00 | 11.83 | 87.00 | 0.04 |
| Anchieta | 4.80 | 20.73 | 35.64 | 82.00 | 0.04 |

$$CN = \frac{5000}{P_0 + 50}$$

where P_0 is the runoff threshold (mm). This is obtained from the land uses and soil types and slope of each basin (Fig. 5): the land uses have been extracted from the Corine Land Cover (2018); the slope has been calculated based on the 5 m Digital Elevation Model (DEM) available

from the IGN (National Geographic Institute); and the soil type has been assigned based on the permeability level indicated in the Soil Permeability Map of Spain made by the Geological and Mining Institute of Spain (IGME for its initials in Spanish) [63]. In this sense, soil type A corresponds to very low permeability, and those with very high permeability have been assigned to group D.)

In turn, the lag time is calculated as [60]:

$$T_{lag} = \frac{L^{0.8} \left(\frac{1000}{CN} - 9 \right)^{0.7}}{1900S^{0.5}}$$

where L is the length of the main watercourse and S, the average slope of the basin. Table 1 shows the parameters for the calculations by basin (Fig. 6).

3.4.3. Flood modeling

HEC-RAS software has been used worldwide in numerous case studies to model and simulate natural watercourses and floods ([64–66], among others). In addition, this software allows carrying out 2D models with the minimum data requirement: the elevation model and the flow [67]. In this sense, the used DEM has a resolution of 5 m and the flow data come from those calculated in the previous section with the HEC-HMS software. Apart from these, another parameter required by the hydraulic model is the channel resistance corresponding to Manning’s coefficient [68]. These were assigned according to the established by the

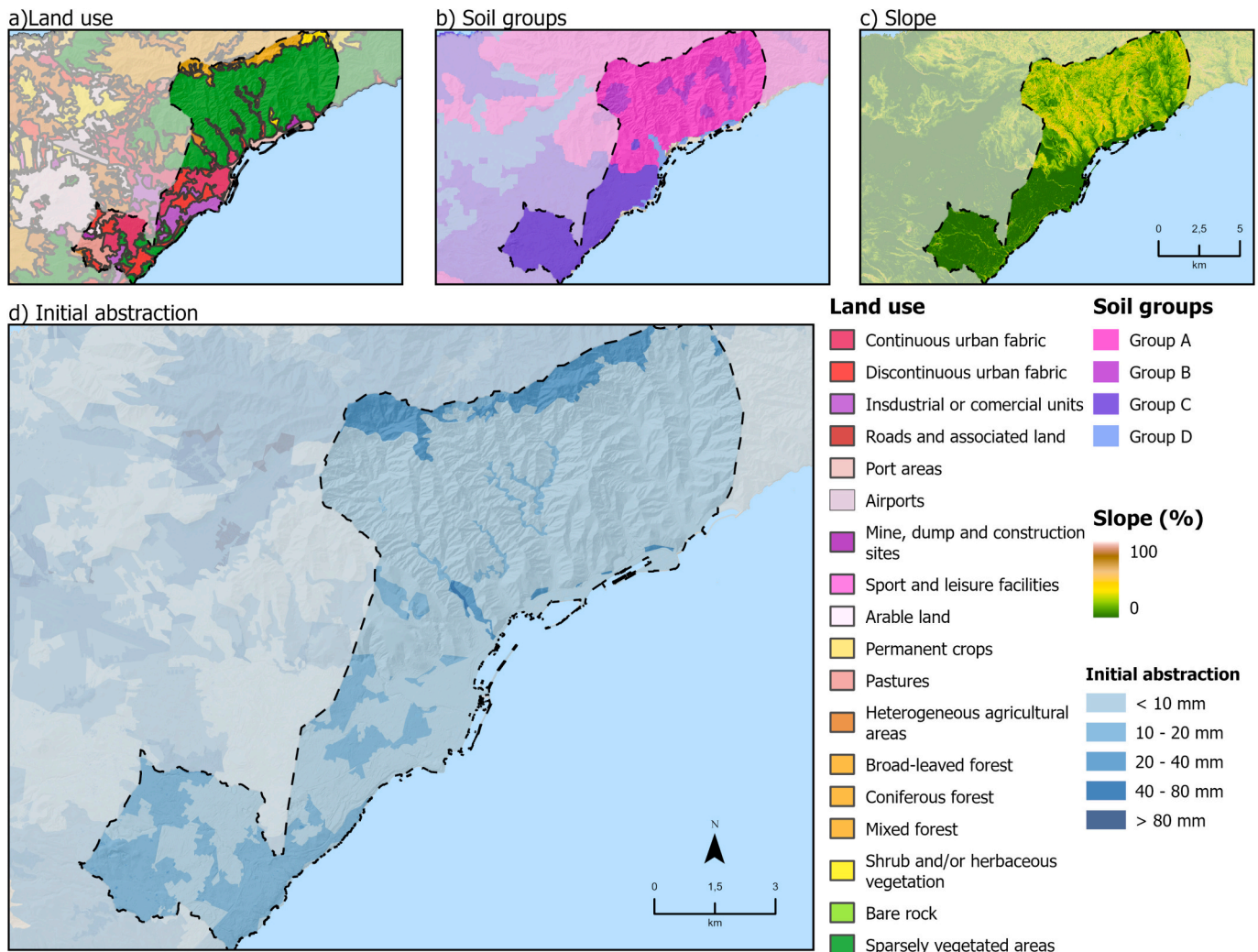


Fig. 5. Runoff threshold of the study area.



Fig. 6. Basins used in the study.

SNCZI based on the land uses of the Corine Land Cover [62]. With all these data, an *unsteady flow analysis* was performed, in which the discharge hydrograph was inserted with a duration of 5 h and divided into 20-min intervals.

3.5. Stage 5. Integration of the factors that characterize the hazard and generation of flood susceptibility mapping

In cities with similar characteristics to those analyzed in this study, the potential damages or impacts of flooding are not only related to problems linked to the hydrographic network. Direct urban runoff also has an enormous influence on the number and magnitude of incidents that occur during an extreme precipitation event. This is related to the high percentage of soil sealing and the poor conditions of water drainage hydraulic infrastructures [69]. Therefore, a good susceptibility analysis should not only pay attention to modeling around watercourses [70]. The analysis of impacts, their characterization and localization during historical events, is key in this type of field to improve the accuracy and quality of flood hazard maps. Thus, in this research, the results obtained from the analysis of incidents and the hydraulic modeling of extreme flows have been adapted in order to integrate both information related to flood hazards.

First, a *kernel* analysis of the identified incidents is performed to establish a classification of the city surface based on hotspot flooding zones that is contained in a raster information layer [71]. The classification is performed through the natural breaks method provided in ArcGIS as a classification choice [72] as it is usually done to establish different hazard levels in risk mitigation analyses [73–75]. This is a data grouping method that seeks to find the best way to organize values into different categories. To achieve this, an attempt is made to minimize the average deviation of each category with respect to its own mean, while maximizing the deviation of each category with respect to the means of the other groups [76]. In this case, the reclassification values would be those shown in Table 2, however, following the natural breaks criterion, these may vary depending on the study area and the results obtained from the kernel analysis. Subsequently, the results of the hydraulic model are added to a raster dataset to which the hazard levels are assigned using the same method to standardize them and allow them to be aggregated with the data resulting from the kernel. Finally, through a map algebra operation, the values of the results of both analyses are added and the result is classified into intervals to form a final flood susceptibility map.

Table 2 Numerical thresholds for reclassification using natural breaks method.

| Analysis kernel reclassification | |
|-------------------------------------|--------------|
| Threshold | Hazard level |
| < 64.4 | 1 |
| 64.4–119.9 | 2 |
| 119.9–197.7 | 3 |
| 197.7–315.4 | 4 |
| > 315.4 | 5 |
| Hydrological model reclassification | |
| < 1 | 1 |
| 1–5 | 2 |
| 5–13 | 3 |
| 13–25 | 4 |
| > 25 | 5 |
| Final classification | |
| 0–1 | 1 |
| 1–2 | 2 |
| 2–4 | 3 |
| 4–5 | 4 |
| > 5 | 5 |

4. Results

The results obtained are presented below in two sections. The first section relates the damage history with its possible causes (methodological stages 1 to 3); the second section presents the results of the hydraulic modeling of the extreme flow scenario and the integration of the information to obtain the flood susceptibility map of the study area (methodological stages 4 to 5).

4.1. Relationship between recorded damage incidents and their possible causes (stage 1 to 3)

In the process of identifying historical modifications to the natural drainage network, a total of 153 watercourses were inventoried, of which 119 are preserved to a greater or lesser extent and 34 have disappeared as a result of urbanization. Of the former, 14 of them are considered main watercourses, with Strahler order of 3–4 and the rest are lower order tributaries (Fig. 7). Among the eliminated 34, two

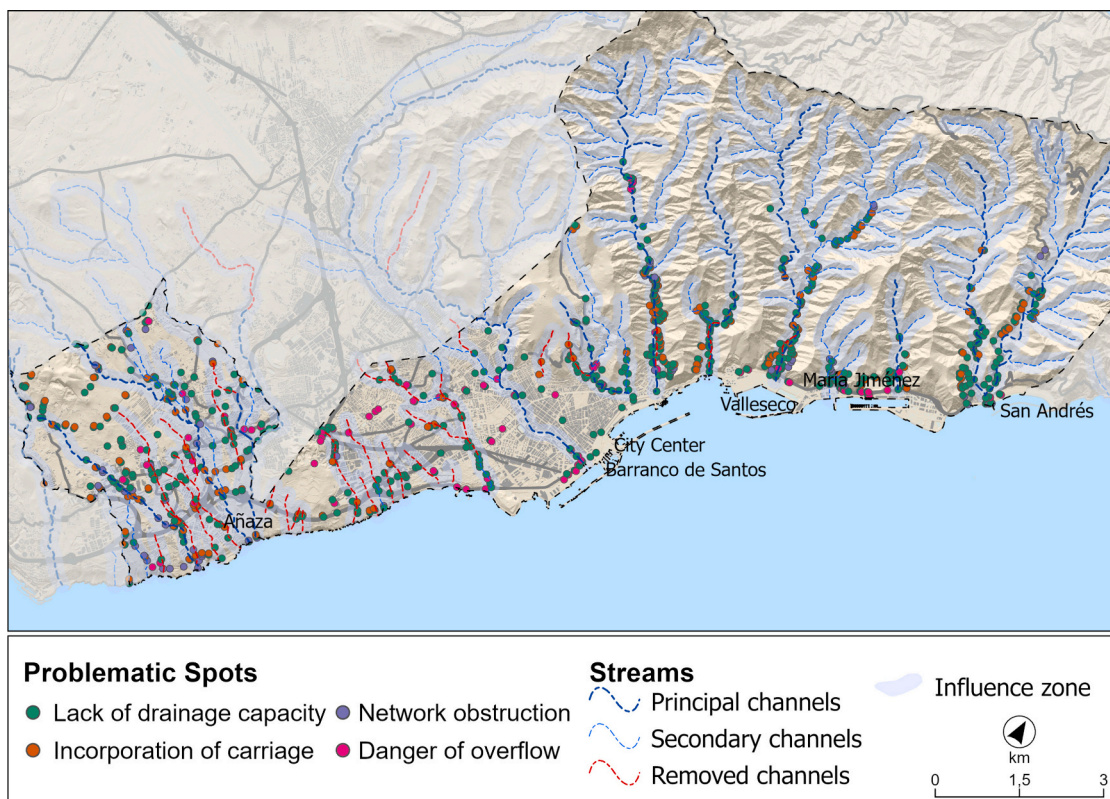


Fig. 7. Damage points identified in the PGO of Santa Cruz de Tenerife classified according to their problematic nature.

groups can be distinguished. On the one hand, there are watercourses that have completely or partially disappeared as a result of urbanization, located in the southwestern and central sectors of the city. Important sections of its suppressed route stand out here, in some cases exceeding one kilometer in length. On the other hand, there are ravines whose course has been altered or diverted, although they have not disappeared. This is the case of the ravines that originate in the interior of the Anaga Massif, which have seen the course of their meanders and/or the interior of their original course altered, being occupied, especially in the sector closest to the mouth.

Regarding the identification of incident points, the study area shows a total of 1023 produced by flooding heterogeneously distributed throughout the municipality. After classification and analysis, two different situations can be observed:

Areas of impact located in the small basins of the former Anaga Massif. In this zone the watercourses are characterized by being well excavated and well defined, where the problem areas are concentrated in the lower section of the basins and on the bed of the watercourse and in the areas near its mouth. These sectors account for 43 % of the incidents.

Areas of impact in the compact urban fabric: where watercourses are much shallower, less marked and defined, and are constrained by the urban fabric. The areas of incidence have a more random and dispersed pattern here. A total of 57 % of the incidents were located in these areas.

These two sectors, mainly due to their high degree of urbanization, are the ones that host important flooding episodes and/or incidents. The high building pressure, together with deficient planning, has resulted in the failure to adequately integrate urban planning into the physical environment. In this way, the construction density, in many cases informal, is the cause of the dismantling and occupation of the aforementioned watercourses. In the southwest, where the hydrographic network was hardly noticeable, it has been completely dismantled; in the south of Anaga, we find entire neighborhoods occupying the space of the watercourses. Moreover, the lack of sufficient drainage

infrastructures to solve the deficiencies caused by urbanization and soil sealing resulting from the implementation of road networks and other urban infrastructures has considerably increased the risk of flooding.

For both areas, the most common problem that generates flooding is the lack or insufficient drainage capacity (62.5 %), followed, at a considerable distance, by the incorporation of sediment (20.3 %) (Table 3).

Taking into account both results, a comparative analysis could be made between watercourses and incidents (Fig. 7) which allowed us to characterize the origin of the flood impact. First, it should be noted that 80 % (817) of the incidents are located within the zone of influence (100 m) of the existing drainage network in 1950 (Table 4). 57.2 % are located near watercourses that persist today, in main watercourses, while 24.6 % are closely located to watercourses that have disappeared. Therefore, only 10.6 % are located near secondary tributaries, corresponding mostly to the highest altitudes of the Anaga massif. It is noteworthy that the other 20 % (206) of the incidents identified are located far from the drainage network, proving the considerable importance of urban runoff.

A more detailed analysis reveals the importance or weight of the missing watercourses in causing flooding problems in the urban sectors of the cities. Of the 119 conserved watercourses, only 53.8 % are linked to some incident, while 94.1 % of the watercourses that have disappeared today are linked to one or more incidents. The mean number of incidents per type of watercourse is 7.7 in the former and 9.4 in the

Table 3
Types and frequency of problems recorded in the study area.

| Description | Total | % |
|------------------------------|-------------|------|
| Lack of drainage capacity | 639 | 62.5 |
| Incorporation of carriage | 208 | 20.3 |
| Drainage network obstruction | 96 | 9.4 |
| Danger of overflow | 80 | 7.8 |
| Total | 1023 | |

Table 4
Location of damage points with regard to the drainage network.

| | | No. | Percentage | Total | Percentage |
|---------------------------|--------------------------|-----|------------|-------|------------|
| Zone of influence (100 m) | Main watercourses | 506 | 57.18 | 817 | 79.86 |
| | Disappeared watercourses | 217 | 24.52 | | |
| | Tributaries | 94 | 10.62 | | |
| Out of zone of influence | | | | 206 | 20.14 |
| Total | | | | 1023 | 100.00 |

latter, with a mean of 1 and 5, respectively (Table 5). That said, it is important to mention that 100 % of the 14 main watercourses have complications of some kind. Regarding the type of problems encountered in each type of watercourse, it appears that there is no significant difference between those conserved and those eliminated. In both cases, the most relevant factor is the lack of or insufficient drainage capacity, followed by the incorporation of sediment and the danger of overflowing in last place. However, the problem related to the lack of drainage is 5 % greater in the areas that used to occupy the watercourses that have now disappeared.

4.2. Hydraulic modeling of the extreme flow scenario and integration of the information to obtain the flood susceptibility map (stages 4 to 5)

4.2.1. Numerical flow modeling for an extreme precipitation scenario

Analyzing the calculated return periods, the maximum expected precipitation in 500 years is 43.21 mm in 10 min and 258.33 mm in 12 h (Table 6). If we convert mm to mm/h, the resulting IDF curves show how precipitation intensity behaves; the highest intensities are 259.23 mm/h in 500 years and progressively decreases to around 20 mm/h at 12 h. It appears that after 360 min there is a break in the line of the IDF curve and the intensity gradually decreases.

The resulting storm hyetograph for 500 years, produced from the IDF curves, shows a 120-min storm in which the maximum precipitation is reached in the first hour of the storm (62.02 mm) (Fig. 8). With a total rainfall of 212.8 mm in the design storm the maximum precipitation is located in the center of the storm with 62.02 mm. Following the methodology of alternating blocks, the rest of the values are alternated in descending order on either side of that maximum. Therefore, it is evident that the most critical moment of the storm is between the first 50 and 90 min, where up to a total of 186 mm could be accumulated. The characteristics of the drainage network in the study area hardly delay the peak flow during the storm. This is around 200–210 min, and the permeability of the soil causes the flow to last up to 10 h after the beginning of the storm. The maximum peak flows are between 30 and 70 m³/s and 480 m³/s (Fig. 9). The former corresponds to small ravines with a small area (1–3 km²) and very small watercourse lengths. In

addition, their degree of urbanization is lower than in other sectors and, therefore, their curve numbers are also lower (Table 1).

The Barranco de Santos (Santos Ravine), located right in the urban core of the city, and being the largest watershed in the municipality (41 km²) reaches its Q500 at 483.9 m³/s, similar to what can be reached by some ephemeral watercourses in the Mediterranean [77–79]. Thus, this basin has caused major problems throughout the history of the city, leading to several historical floods [28]. However, its large size is not the only cause of these disasters, since its watercourse has also been constricted as a result of the city’s urban growth and expansion. The second basin in terms of flow rate is the Barranco del Muerto (Ravine of the Dead), with a Q500 of 293.6 m³/s. This is located in the southwestern sector of the municipality, also in a highly urbanized area. Finally, in third place is the Barranco del Bufadero (Bufadero Ravine), which has a Q500 of 238.1 m³/s. This is another of the watercourses whose problems appear repeatedly when there are significant precipitation episodes. Precisely this watercourse, together with the barranco de Tahodio (Tahodio Ravine), is the one with the highest number of damage points, with a total of 114.

The results of the flood modeling (Fig. 10) show a total of 172 ha with flood hazard, corresponding to 2 % of the area studied. The extension is greater, precisely in the basins with a higher level of urbanization. The Barranco Grande (Grande Ravine or Big Ravine), with 35.1 ha and 4.79 % of its surface area threaten, is the basin with the largest area occupied by floodable zones. Closely behind it is the Barranco del Muerto ravine, with 33 ha occupied by flood hazard. However, it is distributed heterogeneously, affecting small isolated sectors scattered throughout the area, as is the case in several areas of the southwest sector. On the other hand, in the center and southeast of the study area, the main flood zones are located mainly at the mouth of the

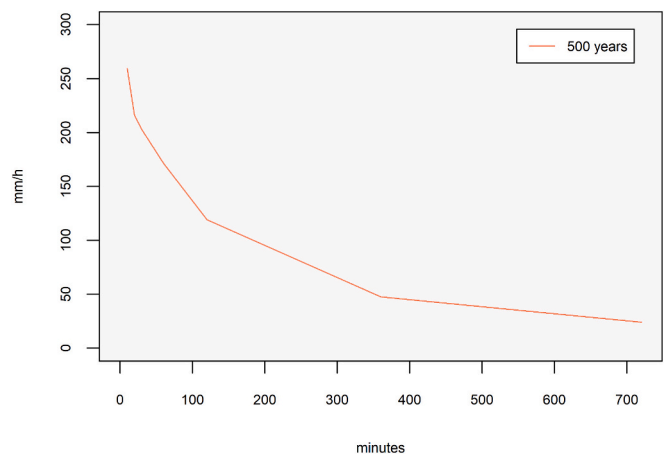


Fig. 8. Santa Cruz de Tenerife IDF curve for a 500-year return period.

Table 5
Summary statistics of watercourses and damage points. It should be noted that several identified points are located within the zone of influence of several watercourses.

| Watercourse type | Watercourses information | | | Incidents statistics | | | | | | |
|------------------|--------------------------|------------------------------------|----------------------------------|----------------------|------|---------|---------|----------|--------------------|--------|
| | No. of watercourses | No. of watercourses with incidents | % of watercourses with incidents | Sum | Mean | Maximum | Minimum | Variance | Standard deviation | Median |
| Current | 119 | 64 | 53.8 | 600 | 7.7 | 99.0 | 0.0 | 215.0 | 14.7 | 1.0 |
| Old | 34 | 32 | 94.1 | 217 | 9.4 | 35.0 | 0.0 | 82.4 | 9.1 | 5.0 |
| Main | 14 | 14 | 100 | 506 | 36.1 | 99.0 | 7.0 | 625.2 | 25.0 | 34.5 |

Table 6
Estimated precipitation for a 500-year return period (mm).

| Minutes | 10 | 20 | 30 | 60 | 120 | 360 | 720 |
|---------|-------|-------|--------|--------|--------|--------|--------|
| T500 | 43.21 | 71.99 | 101.42 | 171.18 | 238.08 | 284.67 | 288.33 |

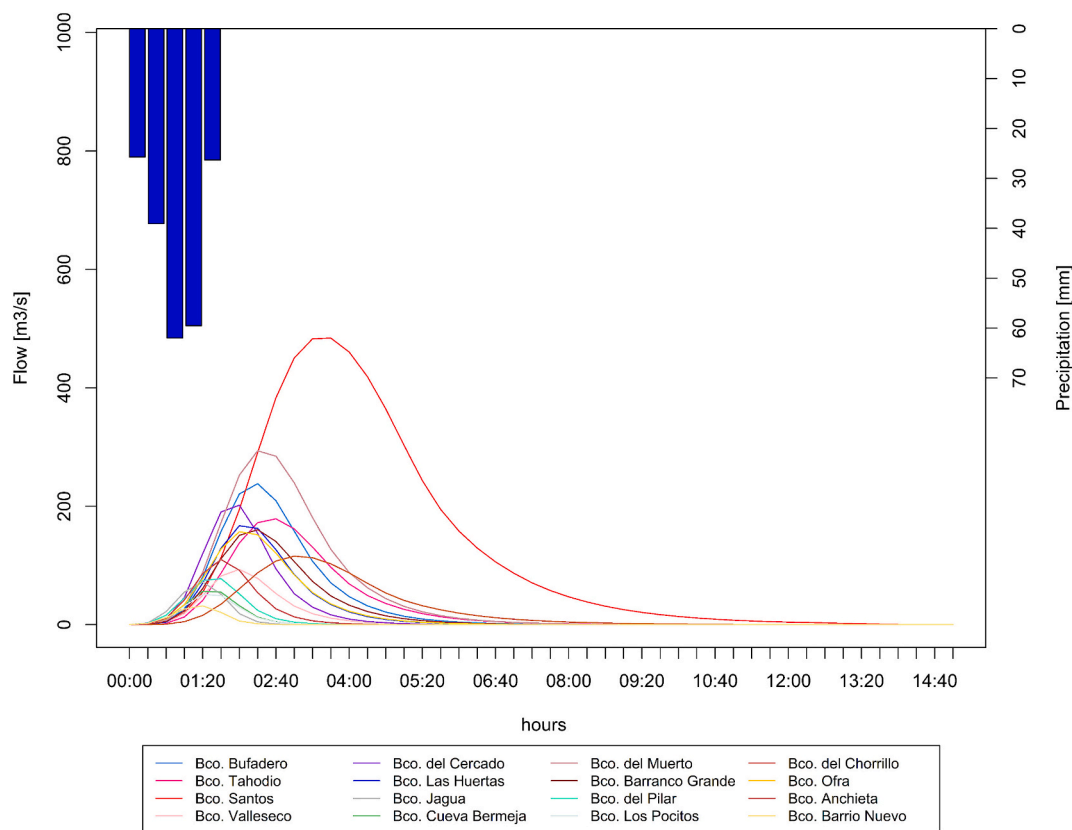


Fig. 9. Hietogram and hydrographs of the studied basins.

watercourses, so that, although they cover a smaller area relative to the basin, the surface area they cover affects more concentrated and highly urbanized sectors.

Of the total number of incidents presented above, only 566 are located within the simulated sectors and of these, 37 % (263) are located in floodable zones. The rest of the points are located outside the defined watercourses of the basins, demonstrating the existence of a clear urban drainage problem. Therefore, the creation of a detailed flood susceptibility map that integrates both variables analyzed in this paper can improve the hazard analysis of the city and the chosen method can serve as an example for other urban areas with similar climatic characteristics. In this sense, the integration of the two variables shows that the areas with the highest hazard are located in the center and southeast of the city (Ofra, Santos, Tahodio and Bufadero Ravines), especially at the mouths (Fig. 11). Incorporating both analyses, the territory susceptible to flooding events is around 16.5 %. Of this percentage 289 ha (19 %) correspond to moderate-high hazard and 314 ha (22.3 %) have a low hazard. In the remaining 57 % of the flooding area, the hazard is very low.

5. Discussion

In urban areas with semi-arid climates, where growth has been exponential, and without territorial planning, it is common for the watercourses of ravines, normally dry, to be occupied [80]. Hence, inventorying and analyzing trouble spots related to flash floods is an issue that has been addressed on numerous occasions [81,82]. The lack or insufficient drainage capacity due to the inadequate construction of drainage works for the maximum flood flow is one of the qualities pointed out for this type of cities [83] that is also identified in Santa Cruz de Tenerife. On the other hand, the incorporation of sediments or solid materials from the slopes, in this case from Anaga, is not only a problem for the drainage network but also for the buildings and infrastructures

located at the foot of the slopes. The obstruction of the drainage network is usually related to both natural objects (roots or rocks) and artificial ones, known as heterometric solids. In addition to all of the above, the implementation of elements in the watercourse itself, such as houses or infrastructures, contribute to the overflowing of the watercourses in the most extreme rainfall events. Considering the importance of these problems in the generation of flood zones, the selection of criteria for the analysis of local factors to improve flood risk management should be related to this. In each of the sectors analyzed, it is necessary to thoroughly investigate the circumstances that have given rise to these problems, in order to identify the factors that are generating them. For example, in this case: the lack of drainage capacity is related to the conditions of the hydraulic infrastructure; the incorporation of carryings and obstruction of the network, with the slope and materials of the basins; and the danger of overflowing, due to the narrowing of the channels by the urban occupation of the basin. Therefore, in order to carry out good actions related to disaster risk reduction, it will not only be necessary to tackle the problems themselves, but also to address those factors that have been identified as the primary causes of the problem.

Currently, there is a multitude of papers aimed at mapping and analyzing flood zones by spatially modeling their expansion, draft and, in some cases, even speed based on different return periods [84–88]. However, to understand and identify areas prone to be affected by flash floods, especially in highly urbanized areas, one must go beyond the analysis of watercourse runoff. A methodology is needed to identify points or sectors with problems and flood zones in order to subsequently carry out the pertinent hazard analyses. Although, as mentioned above, in some cases the problems that cause them have been raised, the complexity of the territory and its temporal dynamism make it necessary to look beyond the current motives.

This study has shown that in urban areas, those prone to flash floods are (1) the ones located in missing watercourses and/or (2) those where a section of the watercourse has been partially modified. In the former,

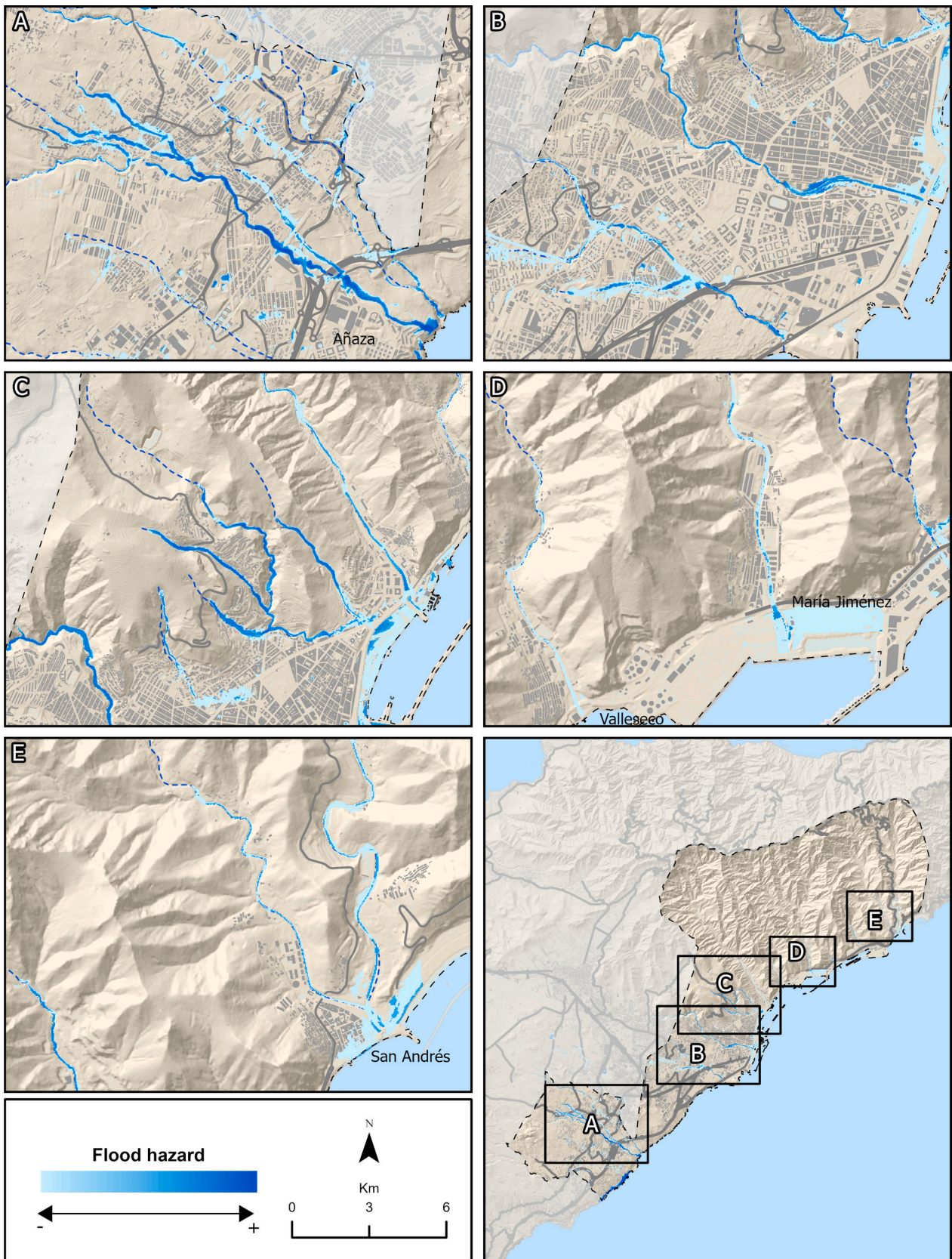


Fig. 10. Flood zones of Santa Cruz de Tenerife.

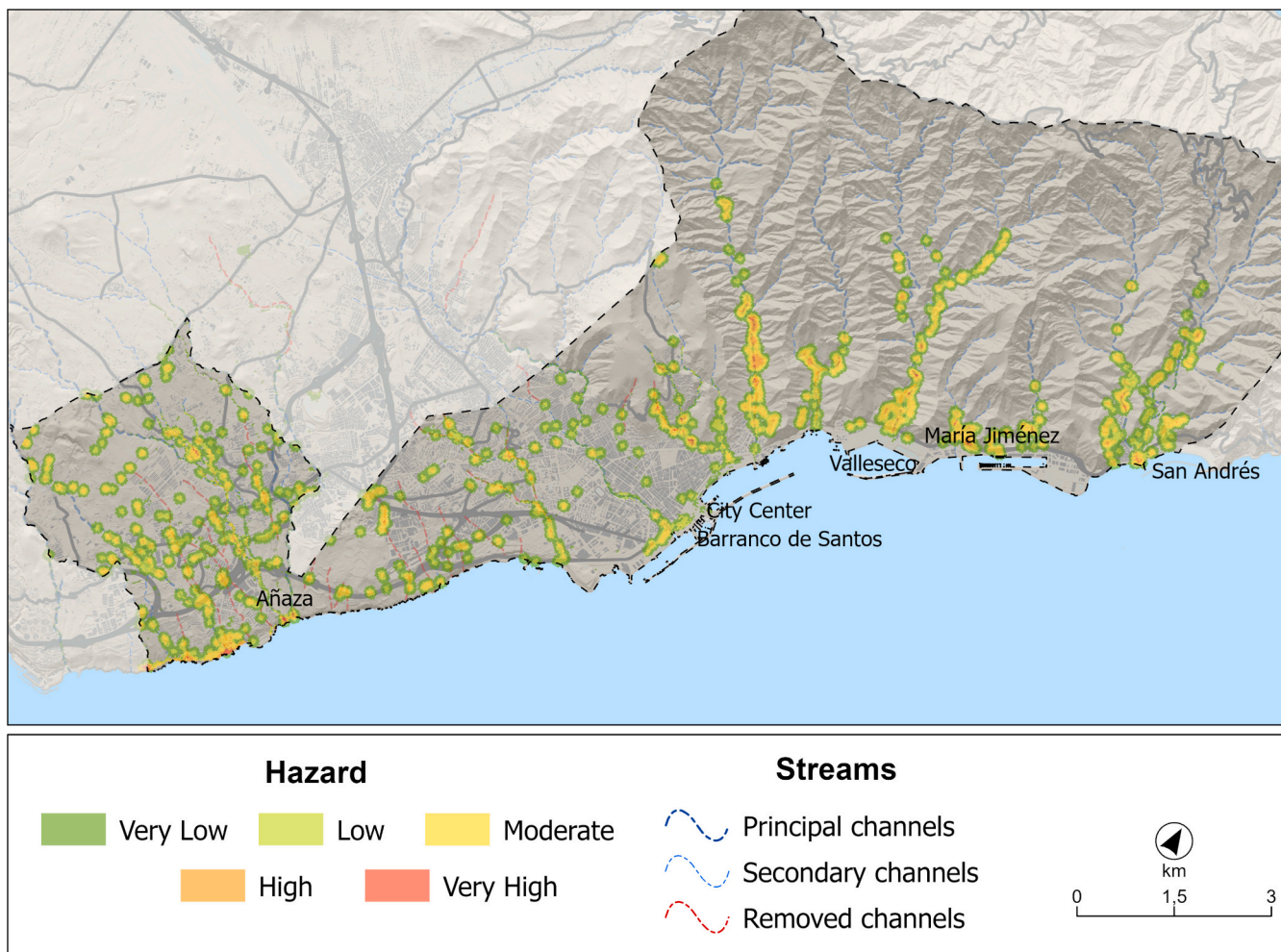


Fig. 11. Flood susceptibility map in Santa Cruz de Tenerife.

as mentioned above, the watercourses eliminated from the drainage network are a key problem and their identification makes it possible to locate risk areas. The location of their trajectories, through images, old maps, or field work, is essential and necessary. However, these are often overlooked and flood susceptibility analyses focus on existing watercourses [89–91]. As for the latter, the watercourse is narrowed and occupied by buildings and infrastructure as a result of urban pressure and the absence of land use planning. In urban areas where growth has been very rapid and unplanned, self-construction around the watercourses of ravines is common, especially among the city’s lower purchasing power classes [10]. This is the case of the Barrancos de María Jiménez and Valleseco (María Jiménez and Valleseco Ravines) in the geographical area analyzed. Therefore, these two typologies of zones should be incorporated into flood risk analyses aimed at planning and disaster risk reduction.

On the other hand, as mentioned above, the identification of problems is complemented with the modeling of flood zones in locations close to the watercourses. In the study area the flow of the ravine depends almost entirely on a precipitation event, since the watercourses are hydrologically disconnected from the aquifers. In the study area, flows are intermittent and remain during long dry periods, similar to what happens in the Mediterranean basin or other semi-arid environments [92]. Similarly, the maximum flows obtained are comparable to those recorded in these environments [93]. In them, the *peak discharge flow* is reached in a very short time interval and the flow rates range from 0 to 100–400 m³/s, subsequently recovering its initial base flow. In this sense, high intensity hourly rainfall and consequent flash floods have

historically generated numerous disasters, especially in highly urbanized sectors [94–97].

As stated by Refsgaard and Hendriksen [98] each hydrological model should be calibrated and validated with datasets representative of the intended domain of applicability. However, the data available for the basins analyzed are extremely limited. Although there are ten-minute rainfall data since 1996, there is still no record of flood flows, not even for extreme events. Therefore, it is impossible to validate the hydrographs obtained with data from historical events. The most useful information available to verify that the hydrological model developed is consistent can be found in the Flood Defence Plan of Tenerife (hereinafter FDC) [99]. Within this plan, an application is developed to calculate the flow of each of the basins for different return periods using the Clark unit hydrograph method [100]. For basins of less than 1km², the rational method is used [101]. Although the values obtained by both studies are not fully comparable due to methodological differences and the fact that the design storm used in the FDC does not have the same duration nor the same temporal distribution pattern - given that in this one the Huff method is used to obtain the hietogram [102] -, it is possible to make an approximate comparison to assess the validity and applicability of the results. As shown in.

Table 7, the flow rates simulated in the present study are close to those simulated in the FDC. When compared using the coefficient of variation, it is observed that the average difference between the two is only 22.2 % and in no case exceeds 45 %. Considering that, in some cases, the discrepancy between the methods used can be as high as 84 % [103], it can be concluded that the model developed is valid and

Table 7
Flow peak discharge simulated and FDC simulation values (CV = coefficient of variation).

| | Simulated | FDC | CV |
|-----------------|-----------|-------|-------|
| Santos | 483,9 | 401 | 13,25 |
| Anchieta | 110 | 70 | 31,43 |
| Barranco Grande | 160,3 | 125,1 | 17,44 |
| Barrio Nuevo | 31,7 | 21,3 | 27,75 |
| Bufadero | 238,1 | 198 | 13,00 |
| Cercado Andrés | 201,8 | 156,8 | 17,75 |
| Chorrillo | 115,6 | 140 | 13,50 |
| Cueva Bermeja | 56,3 | 34,1 | 34,73 |
| | Simulated | FDC | CV |
| Jagua | 72 | 38,4 | 43,04 |
| Las Huertas | 167,1 | 148,3 | 8,43 |
| Los Pocitos | 50,8 | 35,7 | 24,69 |
| Muerto | 293,6 | 193 | 29,24 |
| Ofra | 157 | 101 | 30,70 |
| Pilar | 77,7 | 59,4 | 18,88 |
| Tahodio | 178,7 | 163 | 6,50 |
| Valleseco | 93,3 | 64,1 | 26,24 |

consistent.

Moreover, the highest precipitation event recorded in Santa Cruz de Tenerife took place on March 31, 2002, when 232 mm fell in just two and a half hours, which corresponds to the average annual precipitation in the city. In addition, within the first 120 min of the storm, 188.4 mm had already been recorded (Table 8). It was an event that completely brought the city to a halt, leaving 8 victims, the collapse of basic services (water, electricity and telephone) and substantial economic losses valued at around 200 million euros [37]. Following the calculation of return periods, the data in this paper record a precipitation slightly higher than the one that occurred on that day (280 mm in total), which shows the validity of the return periods and the design storm. When simulating the expected behavior of the watercourses and integrating all the problem areas, the results show a significant relationship with the events of that day in Santa Cruz de Tenerife.

Finally, extraordinary rains with high hourly intensity are, despite their great interannual irregularity, recurrent phenomena in Santa Cruz de Tenerife and, in general, throughout the Canary archipelago [104]. It is important to point out that in the current context of climate change, extreme rainfall events may occur that could modify the level of danger and risk of floods, especially due to the increased risk of the arrival of tropical disturbances [104]. In that sense, globally and from a flood risk management perspective, precipitation intensity on a sub-daily scale is increasing faster than on a daily scale [105]. Given that flash floods are linked to short-duration events it is likely and expected that climate change will have a significant impact on them [106,107]. Santa Cruz de Tenerife is not immune to this phenomenon, and currently there are already studies that confirm the trend of daily concentration of precipitation, increased torrentiality and greater irregularity [108,38]. This would result in an increase in the maximum peak discharge flow and, consequently, in flood zones.

6. Conclusions

Like many cities in the world, Santa Cruz de Tenerife, used as a mere example of methodological application, presents important problems related to urban flooding. As this paper has shown, there are 1023 damage points scattered throughout the city. Lack of or insufficient

Table 8
Accumulated precipitation on March 31, 2002. Source: AEMET.

| Minutes | 10 | 20 | 30 | 60 | 120 | 360 | 720 |
|--------------------|------|----|----|-------|-------|-------|-------|
| Precipitation (mm) | 27.1 | 52 | 75 | 129.9 | 188.4 | 231.2 | 231.4 |

drainage capacity is the most repeated issue. This is related to the construction of insufficient drainage works to evacuate maximum flood flows, highlighting the clear need to combine non-structural quality measures, such as hazard analysis (calculation of return periods and maximum flows), and structural measures (i.e. the construction of drainage works) based on scientific criteria.

On the other hand, the rapid growth of the city, as well as urban planning with many shortcomings, has led to the emergence of settlements in hazardous areas. Using the analyzed case study, the critical role played by urbanization in increasing flood hazards has been confirmed, not only by occupying flood-prone zones, but also by decreasing the runoff threshold due to soil sealing. In this respect, there are two types of sectors in an urban drainage network that are of particular interest from the point of view of flood risk: (1) the main watercourses, since they have peak flows higher than their tributaries; and (2) occupied or dismantled watercourses, since they lack a marked drainage route, and represent sectors with high exposure and vulnerability. This highlights the impact that poor planning or the lack of it has on the occurrence of floods. Not only does it increase exposure and vulnerability to flooding, but it also modifies and amplifies the hazard by creating new sectors susceptible to flooding. For this reason, optimum conservation of watercourses is an important aspect to be taken into account if the risk is to be reduced.

On the other hand, the need for quality data to develop accurate and reliable hydrological models has been emphasized. The lack of data related to floods (precipitation, recorded flows, previously affected areas, etc.) affects the accuracy of predictions and, therefore, risk mitigation strategies based on scientific-technical analyses. Thus, in order to improve the capacity of the models, it would be necessary to establish a consistent and quality monitoring network, at least during those events of a more extraordinary nature, which would provide a good record of data.

In the context of urban flooding, it is of vital interest to know which areas are susceptible in order to ensure the necessary prevention and protection measures for both the population and the territory. Thus, although hydraulic modeling is important, problematic points within the urban fabric must be integrated into the modeling. This is why, in this paper, an integrated susceptibility map has been proposed as a comprehensive alternative to the more traditional flood hazard analyses. This method serves as a first approximation to identify specific zones of interest for more in-depth analyses aimed at disaster risk reduction. In addition, the suggested methodology can be adapted and applied to other urban areas, providing a useful tool for territorial planning.

It should be noted that climate change is expected to accentuate heavy rainfall events, thus increasing the risk of flooding. Therefore, future studies should include climate projections of precipitation to better define maximum flood flows in order to design efficient drainage infrastructures and take appropriate actions to reduce the risk of flood disasters. Finally, this study allows for the possibility of developing new works that incorporate data related to vulnerability and exposure, in order to carry out a complete risk calculation, and to detail the areas at risk in the analyzed area.

CRedit authorship contribution statement

Nerea Martín-Raya: Writing – original draft, Methodology, Conceptualization. **Jaime Díaz-Pacheco:** Writing – review & editing, Supervision, Formal analysis. **Pedro Dorta Antequera:** Writing – review & editing, Supervision, Resources. **Abel López-Díez:** Writing – review & editing, Validation, Funding acquisition.

Declaration of competing interest

The authors declare that they have no known competing financial interests or personal relationships that could have appeared to influence

the work reported in this paper.

Data availability

No data was used for the research described in the article.

Acknowledgements

This research is inserted in the research project “Tools for the prevention and management of floods social impacts in coastal areas (AQUASOC)” funding by the Ministry of Science, Innovation and Universities of Spain.

The first author, Nerea Martín-Raya, received an FPU PhD (FPU21/01343) grant from the Ministry of Science, Innovation and Universities of Spain.

References

- [1] Bui DT, Tsangaratos P, Ngo PTT, Pham TD, Pham BT. Flash flood susceptibility modeling using an optimized fuzzy rule-based feature selection technique and tree-based ensemble methods. *Sci Total Environ* 2019;668:1038–54. <https://doi.org/10.1016/j.scitotenv.2019.02.422>.
- [2] Pham BT, Avand M, Janizadeh S, Phong TV, Al-Ansari N, Ho LS, et al. GIS based hybrid computational approaches for flash flood susceptibility assessment. *Water* 2020;12(3):683. <https://doi.org/10.3390/w12030683>.
- [3] Rosa A, Cardoso C, Vieira R, Faria R, Oliveira AR, Navarro G, et al. Impact of flash flood events on the coastal waters around Madeira Island: the “land mass effect”. *Front Mar Sci* 2022;8:749638. <https://doi.org/10.3389/fmars.2021.749638>.
- [4] Stavropoulos S, Zaimis GN, Filippidis E, Diaconu DC, Emmanoueloudis D. Mitigating flash floods with the use of new technologies: a multi-criteria decision analysis to map flood susceptibility for Zakynthos Island, Greece. *J Urban Reg Anal* 2020;12(2):233–48. <https://doi.org/10.37043/JURA.2020.12.2.7>.
- [5] Alipour A, Ahmadalipour A, Moradkhani H. Assessing flash flood hazard and damages in the Southeast United States. *J Flood Risk Manag* 2020;13(2):e12605. <https://doi.org/10.1111/jfr3.12605>.
- [6] Amengual A, Borga M. Hydrometeorological analysis of an extreme flash-flood: the 28 September 2012 event in Murcia, South-Eastern Spain. In: *Climate change, hazards and adaptation options: handling the impacts of a changing climate*; 2020. p. 3–26. https://doi.org/10.1007/978-3-030-37425-9_1.
- [7] Faccini F, Luino F, Paliaga G, Roccati A, Turconi L. Flash flood events along the west mediterranean coasts: inundations of urbanized areas conditioned by anthropic impacts. *Land* 2021;10(6):620. <https://doi.org/10.3390/land10060620>.
- [8] Wink Junior MV, dos Santos LG, Ribeiro FG, da Trindade CS. Natural disasters and poverty: evidence from a flash flood in Brazil. *Environ Dev Sustain* 2023;1–22. <https://doi.org/10.1007/s10668-023-03623-0>.
- [9] IPCC. *Cambio Climático 2007: Un resumen para todo el mundo*. https://www.ipcc.ch/report/ar6/wg1/downloads/outreach/IPCC_AR6_WGI_SummaryForAll_Sp_anish.pdf; 2021.
- [10] Anwana EO, Owojori OM. Analysis of flooding vulnerability in informal settlements literature: mapping and research agenda. *Soc Sci* 2023;12:40. <https://doi.org/10.3390/socsci12010040>.
- [11] Bathrellos GD, Karymbalis E, Skilodimou HD, Gaki-Papanastassiou K, Baltas EA. Urban flood hazard assessment in the basin of Athens metropolitan city, Greece. *Environ Earth Sci* 2016;75:1–14. <https://doi.org/10.1007/s12665-015-5157-1>.
- [12] Hosseini FS, Choubin B, Mosavi A, Nabipour N, Shamsirband S, Darabi H, et al. Flash-flood hazard assessment using ensembles and Bayesian-based machine learning models: application of the simulated annealing feature selection method. *Sci Total Environ* 2020;711:135161. <https://doi.org/10.1016/j.scitotenv.2019.135161>.
- [13] Kvočka D, Falconer RA, Bray M. Flood hazard assessment for extreme flood events. *Nat Hazards* 2016;84:1569–99. <https://doi.org/10.1007/s11069-016-2501-z>.
- [14] Maranzoni A, D’Oria M, Rizzo C. Quantitative flood hazard assessment methods: a review. *J Flood Risk Manag* 2023;16(1):e12855. <https://doi.org/10.1111/jfr3.12855>.
- [15] Mosquera-Machado S, Ahmad S. Flood hazard assessment of Atrato River in Colombia. *Water Resour Manag* 2007;21:591–609. <https://doi.org/10.1007/s11269-006-9032-4>.
- [16] Robinson A, Lehmann J, Barriopedro D, Rahmstorf S, Coumou D. Increasing heat and rainfall extremes now far outside the historical climate. *npj Clim Atmos Sci* 2021;4(1):45. <https://doi.org/10.1038/s41612-021-00202-w>.
- [17] Boudiaf B, Dabanli I, Boutaghane H, et al. Temperature and precipitation risk assessment under climate change effect in Northeast Algeria. *Earth Syst Environ* 2020. <https://doi.org/10.1007/s41748-019-00136-7>.
- [18] Ogden FL, Pradhan NR, Downer CW, Zahner JA. Relative importance of impervious area, drainage density, width function, and subsurface storm drainage on flood runoff from an urbanized catchment. *Water Resour Res* 2011;47:W12503. <https://doi.org/10.1029/2011WR010550>.
- [19] Shao M, Zhao G, Kao SC, Cuo L, Rankin C, Gao H. Quantifying the effects of urbanization on floods in a changing environment to promote water security—a case study of two adjacent basins in Texas. *J Hydrol* 2020;589:125154. <https://doi.org/10.1016/j.jhydrol.2020.125154>.
- [20] Chen X, Tian C, Meng X, Xu Q, Cui G, Zhang Q, et al. Analyzing the effect of urbanization on flood characteristics at catchment levels. *Proc Int Assoc Hydrol Sci* 2015;370(370):33–8. <https://doi.org/10.5194/piahs-370-33-2015>.
- [21] Du J, Qian L, Rui H, Zuo T, Zheng D, Xu Y, et al. Assessing the effects of urbanization on annual runoff and flood events using an integrated hydrological modeling system for Qinhuai River basin, China. *J Hydrol* 2012;464:127–39. <https://doi.org/10.1016/j.jhydrol.2012.06.057>.
- [22] Feng B, Zhang Y, Bourke R. Urbanization impacts on flood risks based on urban growth data and coupled flood models. *Nat Hazards* 2021;106:613–27. <https://doi.org/10.1007/s11069-020-04480-0>.
- [23] Hejazi MI, Markus M. Impacts of urbanization and climate variability on floods in northeastern Illinois. *J Hydrol Eng* 2009;14(6):606–16. [https://doi.org/10.1061/\(ASCE\)HE.1943-5584.0000020](https://doi.org/10.1061/(ASCE)HE.1943-5584.0000020).
- [24] Nigussie TA, Altunkaynak A. Modeling the effect of urbanization on flood risk in Ayamama watershed, Istanbul, Turkey, using the MIKE 21 FM model. *Nat Hazards* 2019;99:1031–47. <https://doi.org/10.1007/s11069-019-03794-y>.
- [25] Saber M, Abdrabo KI, Habiba OM, Kantosh SA, Sumi T. Impacts of triple factors on flash flood vulnerability in Egypt: urban growth, extreme climate, and mismanagement. *Geosciences* 2020;10(1):24. MDPI AG. Retrieved from, <https://doi.org/10.3390/geosciences10010024>.
- [26] Manawi SMA, Nasir KAM, Shiru MS, Hotaki SF, Sediqi MN. Urban flooding in the northern part of Kabul City: causes and mitigation. *Earth Syst Environ* 2020;4:599–610. <https://doi.org/10.1007/s41748-020-00165-7>.
- [27] Pour SH, Abd Wahab AK, Shahid S, Asaduzzaman M, Dewan A. Low impact development techniques to mitigate the impacts of climate-change-induced urban floods: current trends, issues and challenges. *Sustain Cities Soc* 2020;62:102373. <https://doi.org/10.1016/j.scs.2020.102373>.
- [28] Marzol MV. Lluvias e inundaciones en la ciudad de Santa Cruz de Tenerife. In: *Publicaciones de la Asociación Española de Climatología. Serie A*; 2002. p. 3. <http://hdl.handle.net/20.500.11765/9171>.
- [29] Khosravi K, Pourghasemi HR, Chapi K, Bahri M. Flash flood susceptibility analysis and its mapping using different bivariate models in Iran: a comparison between Shannon’s entropy, statistical index, and weighting factor models. *Environ Monit Assess* 2016;188:1–21. <https://doi.org/10.1007/s10661-016-5665-9>.
- [30] Rahmati O, Pourghasemi HR, Zeinivand H. Flood susceptibility mapping using frequency ratio and weights-of-evidence models in the Golan Province, Iran. *Geocarto Int* 2016;31:42–70. <https://doi.org/10.1080/10106049.2015.1041559>.
- [31] Bult DT, Abebe BG. A review of flood modeling methods for urban pluvial flood application. *Model Earth Syst Environ* 2020. <https://doi.org/10.1007/s40808-020-00803-z>.
- [32] Devi GK, Ganasri BP, Dwarakish GS. A review on hydrological models. *Aquat Procedia* 2015;4:1001–7. <https://doi.org/10.1016/j.aqpro.2015.02.126>.
- [33] Anees MT, Abdullah K, Nordin MNM, Rahman NNNA, Syakir MI, Kadir MO A. One- and two-dimensional hydrological modelling and their uncertainties. *Intech* 2017;38. <https://doi.org/10.1016/j.colsurfa.2011.12.014>.
- [34] Mudashiru RB, Sabtu N, Abustan I, Balogun W. Flood hazard mapping methods: a review. *J Hydrol* 2021;603:126846. <https://doi.org/10.1016/j.jhydrol.2021.126846>.
- [35] Ministerio de transición ecológica. *Áreas con riesgo potencial significativo de inundación. Cartografía digital*; 2023. Available at: <https://www.miteco.gob.es/es/cartografia-y-sig/ide/descargas/agua/arspi.html>.
- [36] *Calabdo de Tenerife. Plan de gestión de riesgo de inundación de Tenerife. In: Ciclo de planificación hidrológica 2021–2027. Memoria*; 2023.
- [37] López Díez A, Dorta P, Díaz Pacheco J, Caraballo Acosta O. Consecuencias de los eventos meteorológicos de rango extraordinario en Canarias: temporales de viento, inundaciones y fenómenos costeros (1996–2016). <http://hdl.handle.net/20.500.11765/9953>; 2018.
- [38] Máyer P, Marzol MW, Parreño Castellano JM. Precipitation trends and a daily precipitation concentration index for the mid-eastern Atlantic (Canary Islands, Spain). In: *Cuadernos de Investigación Geográfica*; 2017. <https://doi.org/10.18172/cig.3095>.
- [39] Martín-Vide J. Spatial distribution of a daily precipitation concentration index in peninsular Spain. *Int J Climatol* 2004;24(8):959–71. <https://doi.org/10.1002/joc.1030>.
- [40] Máyer P, Marzol V. Daily precipitation concentration and the rainy spells in the Canary Islands: two risk factors. *Bol Asoc Geógr Esp* 2014;65:436–68.
- [41] *Ayuntamiento Santa Cruz de Tenerife. Plan General de Ordenación. In: Estudio de Riesgos Tomo I.2*; 2013.
- [42] Solin L, Skubincan P. Flood risk assessment and management: review of concepts, definitions and methods. *Geogr J* 2013;65:23–44.
- [43] Dasallas L, Kim Y, An H. Case study of HEC-RAS 1D–2D coupling simulation: 2002 Baeksan flood event in Korea. *Water* 2019;11(10):2048. <https://doi.org/10.3390/w11102048>.
- [44] García-Feal O, González-Cao J, Gómez-Gesteira M, Cea L, Domínguez JM, Formella A. An accelerated tool for flood modelling based on Iber. *Water* 2018;10(10):1459. <https://doi.org/10.3390/w10101459>.
- [45] Ongdas N, Akiyanova F, Karakulov Y, Muratbayeva A, Zinabdin N. Application of HEC-RAS (2D) for flood hazard maps generation for Yesil (Ishim) river in Kazakhstan. *Water* 2020;12(10):2672. <https://doi.org/10.3390/w12102672>.
- [46] Costache R, Barbulescu A, Pham QB. Integrated framework for detecting the areas prone to flooding generated by flash-floods in small river catchments. *Water* 2021;13(6):758. <https://doi.org/10.3390/w13060758>.

- [47] Ma Y, Cui Y, Tan H, Wang H. Case study: diagnosing China's prevailing urban flooding—causes, challenges, and solutions. *J Flood Risk Manag* 2022;15(3): e12822. <https://doi.org/10.1111/jfr3.12822>.
- [48] Majumder R, Bhunia GS, Patra P, Mandal AC, Ghosh D, Shit PK. Assessment of flood hotspot at a village level using GIS-based spatial statistical techniques. *Arab J Geosci* 2019;12(13):409. <https://doi.org/10.1007/s12517-019-4558-y>.
- [49] Müller A, Reiter J, Weiland U. Assessment of urban vulnerability towards floods using an indicator-based approach—a case study for Santiago de Chile. *Nat Hazards Earth Syst Sci* 2011;11(8):2107–23. <https://doi.org/10.5194/nhess-11-2107-2011>.
- [50] Perles Roselló, M.J., Olcina, J., Mérida Rodríguez, M., Balance de las políticas de gestión del riesgo de inundaciones en España: de las acciones estructurales a la ordenación territorial. Available at: <https://rua.ua.es/dspace/handle/10045/89637>, 2018.
- [51] El-Fakharany MA, Mansour NM. Morphometric analysis and flash floods hazards assessment for Wadi Al Aawag drainage basins, Southwest Sinai, Egypt. *Environ Earth Sci* 2021;80:1–17. <https://doi.org/10.1007/s12665-021-09457-1>.
- [52] Dupigny-Giroux LA, Goff J, Kilbride J, Marshall JD, Leidinger S, Fooks P, et al. Improving situational awareness for flash flood forecasting in a small urban catchment by integrating meteorological analysis into a geospatial framework. *Remote Sens Appl Soc Environ* 2019;14:224–38. <https://doi.org/10.1016/j.rsase.2017.09.003>.
- [53] de Albuquerque AO, de Carvalho Júnior OA, Guimarães RF, Gomes RAT, Hermuche PM. Assessment of gully development using geomorphic change detection between pre-and post-urbanization scenarios. *Environ Earth Sci* 2020; 79(10):232. <https://doi.org/10.1007/s12665-020-08958-9>.
- [54] IGN. Documentación Geográfica y Cartografías Antiguas. Minutas MTN50. Centro de descargas del Instituto Geográfico Nacional; 2023. Available at: <https://centrodedescargas.cnig.es/CentroDescargas/index.jsp>.
- [55] Gobierno de España Minutas del Mapa Topográfico Nacional 1:50.000 (1915–1960) - Conjunto de datos. <https://datos.gob.es/es/catalogo/e00125901-spaingminutasmtn50>; 1960.
- [56] Cherqui F, Belmeziti A, Granger D, Sourdiril A, Le Gauffre P. Assessing urban potential flooding risk and identifying effective risk-reduction measures. *Sci Total Environ* 2015;514:418–25. <https://doi.org/10.1016/j.scitotenv.2015.02.027>.
- [57] PGO. Plan General de Ordenación de Santa Cruz de Tenerife. Ayuntamiento de Santa Cruz de Tenerife. Available at: <https://www.urbanismosantacruz.es/sites/default/files/Planeamiento/AB-PGOU92/BOC29-06.pdf>; 2005.
- [58] Teng J, Jakeman AJ, Vaze J, Croke BF, Dutta D, Kim SJEM. Flood inundation modelling: a review of methods, recent advances and uncertainty analysis. *Environ Model Software* 2017;90:201–16. <https://doi.org/10.1016/j.envsoft.2017.01.006>.
- [59] Bezak N, Šraj M, Mikoš M. Copula-based IDF curves and empirical rainfall thresholds for flash floods and rainfall-induced landslides. *J Hydrol* 2016;541: 272–84. <https://doi.org/10.1016/j.jhydrol.2016.02.058>.
- [60] Shatnawi A, Ibrahim M. Derivation of flood hydrographs using SCS synthetic unit hydrograph technique for Housha catchment area. *Water Supply* 2022;22(5): 4888–901.
- [61] Pratama MI, Rohmat FIW, Farid M, Adityawan MB, Kuntoro AA, Moe IR. Flood hydrograph simulation to estimate peak discharge in Ciliwung river basin. In: IOP conference series: Earth and environmental science (Vol. 708, No. 1). IOP Publishing; 2021, April, 012028. <https://doi.org/10.1088/1755-1315/708/1/012028>.
- [62] Ministerio para la Transición Ecológica, MITECO. Guía Metodológica Para el Desarrollo del Sistema Nacional de Cartografía de Zonas Inundables. 1st ed. Madrid, Spain: Ministerio de Medio Ambiente y Medio Rural y Marino; 2011. p. 19–52.
- [63] del Pozo Gómez M (Coord). Mapa Litoestratigráfico, de Permeabilidad e Hidrogeológico de España continuo digital a escala 1:200.000. In: Convenio de colaboración entre el Ministerio de Medio Ambiente y el Instituto Geológico y Minero de España para la realización de trabajos técnicos en relación con la aplicación de la Directiva Marco del Agua en materia de agua subterránea. Madrid: IGME; 2009.
- [64] Khattak MS, Anwar F, Saeed TU, Sharif M, Sheraz K, Ahmed A. Floodplain mapping using HEC-RAS and ArcGIS: a case study of Kabul River. *Arab J Sci Eng* 2016;41:1375–90.
- [65] Knebl MR, Yang ZL, Hutchison K, Maidment DR. Regional scale flood modeling using NEXRAD rainfall, GIS, and HEC-HMS/RAS: a case study for the San Antonio River basin summer 2002 storm event. *J Environ Manage* 2005;75(4):325–36. <https://doi.org/10.1016/j.jenvman.2004.11.024>.
- [66] Ogras S, Onen F. Flood analysis with HEC-RAS: a case study of Tigris River. *Adv Civ Eng* 2020;2020:1–13. <https://doi.org/10.1155/2020/6131982>.
- [67] Rangari VA, Umamahesh NV, Bhatt CM. Assessment of inundation risk in urban floods using HEC RAS 2D. *Model Earth Syst Environ* 2019;5:1839–51. <https://doi.org/10.1007/s40808-019-00641-8>.
- [68] Hicks FE, Peacock T. Suitability of HEC-RAS for flood forecasting. *Can Water Res J* 2005;30(2):159–74. <https://doi.org/10.4296/cwrj3002159>.
- [69] Li C, Liu M, Hu Y, Shi T, Qu X, Walter MT. Effects of urbanization on direct runoff characteristics in urban functional zones. *Sci Total Environ* 2018;643:301–11. <https://doi.org/10.1016/j.scitotenv.2018.06.211>.
- [70] Walsh CJ, Fletcher TD, Burns MJ. Urban stormwater runoff: a new class of environmental flow problem. 2012. <https://doi.org/10.1371/journal.pone.0045814>.
- [71] Zhang H, Jia H, Liu W, Wang J, Xu D, Li S, et al. Spatiotemporal information mining for emergency response of urban flood based on social media and remote sensing data. *Remote Sens (Basel)* 2023;15(17):4301. <https://doi.org/10.3390/rs15174301>.
- [72] Rahadianto H, Fariza A, Hasim JAN. Risk-level assessment system on Bengawan Solo River basin flood prone areas using analytic hierarchy process and natural breaks: study case: East Java. In: 2015 international conference on data and software engineering (ICoDSE). IEEE; 2015, November. p. 195–200. <https://doi.org/10.1109/ICoDSE.2015.7436997>.
- [73] Iglesias V, Braswell AE, Rossi MW, Joseph MB, McShane C, Cattau M, et al. Risky development: increasing exposure to natural hazards in the United States. *Earth's Future* 2021;9(7). <https://doi.org/10.1029/2020EF001795>. e2020EF001795.
- [74] Simpson DM, Human RJ. Large-scale vulnerability assessments for natural hazards. *Nat Hazards* 2008;47:143–55. <https://doi.org/10.1007/s11069-007-9202-6>.
- [75] Ullah K, Zhang J. GIS-based flood hazard mapping using relative frequency ratio method: a case study of Panjkora River basin, eastern Hindu Kush, Pakistan. *PLoS One* 2020;15(3):e0229153. <https://doi.org/10.1371/journal.pone.0229153>.
- [76] Fariza A, Abhimata NP, Hasim JAN. Earthquake disaster risk map in East Java, Indonesia, using analytical hierarchy process—natural break classification. In: 2016 international conference on knowledge creation and intelligent computing (KCIC). IEEE; 2016, November. p. 141–7. <https://doi.org/10.1109/KCIC.2016.7883638>.
- [77] Belmonte AMC, Beltrán FS. Flood events in Mediterranean ephemeral streams (ramblas) in Valencia region, Spain. *Catena* 2001;45(3):229–49. [https://doi.org/10.1016/S0341-8162\(01\)00146-1](https://doi.org/10.1016/S0341-8162(01)00146-1).
- [78] Benito G, Sanchez-Moya Y, Medialdea A, Barriendos M, Calle M, Rico M, et al. Extreme floods in small mediterranean catchments: long-term response to climate variability and change. *Water* 2020;12(4):1008. <https://doi.org/10.3390/w12041008>.
- [79] Rinat Y, Marra F, Zoccatelli D, Morin E. Controls of flash flood peak discharge in Mediterranean basins and the special role of runoff-contributing areas. *J Hydrol* 2018;565:846–60. <https://doi.org/10.1016/j.jhydrol.2018.08.055>.
- [80] Pino A, Hormazábal N. Informal settlements: Reinterpreting rural imaginary in urban areas: The case of Valparaíso's ravines. *Habitat Int* 2016;53:534–45. <https://doi.org/10.1016/j.habitatint.2015.12.014>.
- [81] López Díez A, Díaz Pacheco JS, Dorta Antequera P, Máyer Suárez PL. La evaluación del riesgo de inundación en el contexto local de adaptación al cambio climático. El caso de la isla de Tenerife. In: Estudios Geográficos; 2021. <https://doi.org/10.3989/estgeogr.202190.090>.
- [82] Marlow D, Pearson L, MacDonald DH, Whitten S, Burn S. A framework for considering externalities in urban water asset management. *Water Sci. Technol.* 2011;64(11):2199–206.
- [83] Hassan BT, Yassine M, Amin D. Comparison of urbanization, climate change, and drainage design impacts on urban flashfloods in an arid region: case study, New Cairo, Egypt. *Water* 2022;14(15):2430. <https://doi.org/10.3390/w14152430>.
- [84] Anni AH, Cohen S, Praskiewicz S. Sensitivity of urban flood simulation to stormwater infrastructure and soil infiltration. *J Hydrol* 2020;588:125028. <https://doi.org/10.1016/j.jhydrol.2020.125028>.
- [85] Bao H, Wang L, Zhang K, Li Z. Application of a developed distributed hydrological model based on the mixed runoff generation model and 2D kinematic wave flow routing model for better flood forecasting. *Atmos Sci Lett* 2017;18(7):284–93. <https://doi.org/10.1002/asl.754>.
- [86] Luo P, Luo M, Li F, Qi X, Huo A, Wang Z, et al. Urban flood numerical simulation: research, methods and future perspectives. *Environ Model Software* 2022;156: 105478. <https://doi.org/10.1016/j.envsoft.2022.105478>.
- [87] Meng X, Zhang M, Wen J, Du S, Xu H, Wang L, et al. A simple GIS-based model for urban rainstorm inundation simulation. *Sustainability* 2019;11(10):2830. <https://doi.org/10.3390/su11102830>.
- [88] Chang LC, Liou JY, Chang FJ. Spatial-temporal flood inundation nowcasts by fusing machine learning methods and principal component analysis. *J Hydrol* 2022;612:128086. <https://doi.org/10.1016/j.jhydrol.2022.128086>.
- [89] Arabameri A, Seyed Danesh A, Santosh M, Cerda A, Chandra Pal S, Ghorbanzadeh O, et al. Flood susceptibility mapping using meta-heuristic algorithms. *Geomat Nat Haz Risk* 2022;13(1):949–74. <https://doi.org/10.1080/19475705.2022.2060138>.
- [90] Li Y, Hong H. Modelling flood susceptibility based on deep learning coupling with ensemble learning models. *J Environ Manage* 2023;325:116450. <https://doi.org/10.1016/j.jenvman.2022.116450>.
- [91] Seleem O, Ayzel G, de Souza ACT, Bronstert A, Heistermann M. Towards urban flood susceptibility mapping using data-driven models in Berlin, Germany. *Geomat Nat Haz Risk* 2022;13(1):1640–62. <https://doi.org/10.1080/19475705.2022.2097131>.
- [92] Camarasa-Belmonte AM. Flash floods in Mediterranean ephemeral streams in Valencia region (Spain). *J Hydrol* 2016;541:99–115. <https://doi.org/10.1016/j.jhydrol.2016.03.019>.
- [93] Estrany J, Garcia C, Alberich R. Streamflow dynamics in a Mediterranean temporary river. *Hydrol Sci J* 2010;55(5):717–36. <https://doi.org/10.1080/02626667.2010.493740>.
- [94] Curebal I, Efe R, Ozdemir H, Soykan A, Sönmez S. GIS-based approach for flood analysis: case study of Keçidere flash flood event (Turkey). *Geocarto Int* 2016;31(4):355–66. <https://doi.org/10.1080/10106049.2015.1047411>.
- [95] Diakakis M, Andreadakis E, Nikolopoulos EI, Spyrou NI, Gogou ME, Deligiannakis G, et al. An integrated approach of ground and aerial observations in flash flood disaster investigations. The case of the 2017 Mandra flash flood in Greece. *Int J Disaster Risk Reduct* 2019;33:290–309. <https://doi.org/10.1016/j.ijdrr.2018.10.015>.

- [96] Ortega JA, Heydt GG. Geomorphological and sedimentological analysis of flash-flood deposits: the case of the 1997 Rivillas flood (Spain). *Geomorphology* 2009; 112(1–2):1–14. <https://doi.org/10.1016/j.geomorph.2009.05.004>.
- [97] Vinet F. Geographical analysis of damage due to flash floods in southern France: the cases of 12–13 November 1999 and 8–9 September 2002. *Appl Geogr* 2008;28(4):323–36. <https://doi.org/10.1016/j.apgeog.2008.02.007>. Get rights and content.
- [98] Refsgaard JC, Henriksen HJ. Modelling guidelines—terminology and guiding principles. *Adv Water Resour* 2004;27(1):71–82. <https://doi.org/10.1016/j.advwatres.2003.08.006>.
- [99] CIATF. Plan de defensa frente a avenidas. Consejo Insular de Aguas de Tenerife. Available in: [https://aguastenerife.org/8_PDA/PDF/PDA%20completo%20\(Planos%20calidad%20media\).pdf](https://aguastenerife.org/8_PDA/PDF/PDA%20completo%20(Planos%20calidad%20media).pdf); 2005.
- [100] Ahmad MM, Ghumman AR, Ahmad S. Estimation of Clark's instantaneous unit hydrograph parameters and development of direct surface runoff hydrograph. *Water Resour Manag* 2009;23:2417–35. [https://doi.org/10.1061/\(ASCE\)0733-9429\(1988\)114:1\(103\)](https://doi.org/10.1061/(ASCE)0733-9429(1988)114:1(103)).
- [101] Pirozzi J, Ashraf M, Rahman A, Haddad K. Design flood estimation for ungauged catchments in eastern NSW: evaluation of the probabilistic rational method. In: H2009: 32nd hydrology and water resources symposium, Newcastle: adapting to change. Barton, ACT: Engineers Australia; 2009, January. p. 805–16. <https://doi.org/10.3316/informit.755754295380951>.
- [102] Bezak N, Šraj M, Rusjan S, Mikoš M. Impact of the rainfall duration and temporal rainfall distribution defined using the huff curves on the hydraulic flood modelling results. *Geosciences* 2018;8(2):69. <https://doi.org/10.3390/geosciences8020069>.
- [103] Genereux DP. Comparison of methods for estimation of 50-year peak discharge from a small, rural watershed in North Carolina. *Environ Geol* 2003;44:53–8. <https://doi.org/10.1007/s00254-002-0734-5>.
- [104] Dorta P, López A, Díaz J, Máyer P, Romero C. Turismo y amenazas de origen natural en la Macaronesia. Análisis comparado. In: *Cuadernos de turismo*. 45; 2020. p. 61–92.
- [105] Westra S, Fowler H, Evans J, Alexander L, Berg P, Johnson F, et al. Future changes to the intensity and frequency of short-duration extreme rainfall. *Rev Geophys* 2014;52:522–55. <https://doi.org/10.1002/2014RG000464>.
- [106] Prein AF, Rasmussen RM, Ikeda K, Liu C, Clark MP, Holland GJ. The future intensification of hourly precipitation extremes. *Nat Clim Change* 2017;7:48–52. <https://doi.org/10.1038/nclimate3168>.
- [107] Zhang Y, Wang Y, Chen Y, Xu Y, Zhang G, Lin Q, et al. Projection of changes in flash flood occurrence under climate change at tourist attractions. *J Hydrol* 2021; 595:126039. <https://doi.org/10.1016/j.jhydrol.2021.126039>.
- [108] López Díez A, Máyer Suárez P, Díaz Pacheco J, Dorta Antequera P. Rainfall and flooding in coastal tourist areas of the Canary Islands (Spain). *Atmosphere* 2019; 10(12):809. <https://doi.org/10.3390/atmos10120809>.